



# Effect of laser parameters on sequential laser beam micromachining and micro electro-discharge machining

Mir Akmam Noor Rashid<sup>1</sup> · Tanveer Saleh<sup>1</sup> · Wazed Ibne Noor<sup>1</sup> · Mohamed Sultan Mohamed Ali<sup>2</sup>

Received: 21 October 2020 / Accepted: 15 March 2021 / Published online: 20 March 2021  
© The Author(s), under exclusive licence to Springer-Verlag London Ltd., part of Springer Nature 2021

## Abstract

Laser beam micromachining (LBMM) and micro electro-discharge machining ( $\mu$ EDM) based sequential micromachining technique, LBMM- $\mu$ EDM, has drawn significant research attention to utilize the advantages of both methods, i.e., LBMM and  $\mu$ EDM. In this process, a pilot hole is machined by the LBMM, and subsequently finishing operation of the hole is carried out by the  $\mu$ EDM. This paper presents an experimental investigation on the stainless steel (type SS304) to observe the effects of laser input parameters (namely, laser power, scanning speed, and pulse frequency) on the performance of the finishing technique, that is, the  $\mu$ EDM in this case. The scope of the work is limited to 1-D machining, i.e., drilling microholes. It was found that laser input parameters mainly scanning speed and power influenced the output performance of  $\mu$ EDM significantly. Our study suggests that if an increased scanning speed at a lower laser power is used for the pilot hole drilling by the LBMM process, it could result in significantly slower  $\mu$ EDM machining time. On the contrary, if the higher laser power is used with even the highest scanning speed for the pilot hole drilling, then  $\mu$ EDM processing time was faster than the previous case. Similarly,  $\mu$ EDM time was also quicker for LBMMed pilot holes machined at low laser power and slow scanning speed. Our study confirms that LBMM- $\mu$ EDM-based sequential machining technique reduces the machining time, tool wear, and instability (in terms of short circuit count) by a margin of 2.5 x, 9 x, and 40 x, respectively, in contrast to the pure  $\mu$ EDM process without compromising the quality of the holes.

**Keywords** Sequential micromachining · Laser beam micromachining · Micro electro-discharge machining · LBMM ·  $\mu$ EDM

## 1 Introduction

Micromachining is one of the key technologies that has been developed to meet the challenges posed by the requirement of product miniaturizations. Various micromachining techniques are used to create intricate parts in a dimensional range of less than 100  $\mu$ m with tolerance and average surface roughness of sub-micrometer in electronics, aerospace, biomedical, MEMS (micro electromechanical system), and optical industries [1]. Broadly, micromachining can be classified into two major categories, namely, beam-based and tool-based

micromachining. Laser beam, ion beam, photolithography, and electron beam micromachining are examples of beam-based micromachining. In contrast, micro electro-discharge machining, micro electrochemical machining, micro-milling, etc. are examples of tool-based micromachining [2, 3]. According to Chavoshi et al. [1], micromachining has successfully produced complex microstructure (both 2D and 3D) on a broader range of materials with a high level of precision, thus bridging the gap between macro- and microdomain.

Laser beam micromachining (LBMM) is a beam-based machining process that uses thermal energy to carry out the material removal to produce the desired cavity on the workpiece. Due to conventional machining methods' various limitations, LBMM is widely used for drilling, cutting, milling, grooving, turning, etc. [4]. LBMM is a quick machining process; however, its ability of fast material removal comes with the price of the heat-affected zone (HAZ) [4] and forms inaccuracy on the machined feature; i.e., laser micromachining causes the structures to be

✉ Tanveer Saleh  
tanveers@iium.edu.my

<sup>1</sup> Autonomous Systems and Robotics Research Unit (ASRRU), Department of Mechatronics Engineering, International Islamic University Malaysia, 53100 Kuala Lumpur, Malaysia

<sup>2</sup> School of Electrical Engineering, Universiti Teknologi Malaysia, 81310 UTM, Johor Bahru, Johor, Malaysia

tapered [5]. The use of ultrashort pulse laser machining may counteract the problem of HAZ. Ancona et al. [6] used an ultrashort laser beam (1030 nm) with a pulse on time of 800 fs to 19 ps and a repetition rate of 200 to 300 kHz to drill stainless steel plate (thickness = 0.5mm). Yet the holes resulted in the research [6] had a low circularity and substantial recast layer. Gruner et al. [7] used 1030 nm laser beam with 220 fs pulse on time and frequency 10 kHz to 1 MHz to drill thru 0.3 mm stainless steel. The morphological study [7] suggests that the circularity of the holes were somewhat inadequate. Barthels et al. [8] also carried out laser drilling of 10 $\mu$ m stainless steel sheet using 900 fs laser (515 nm) with a repetition frequency 100 kHz. The microscopic study suggests that the holes are not free from the heat-affected zone [8]. However, researchers also reported that with optimum processing condition, the ultrashort laser can produce precise microholes with reasonable dimensional accuracy and reduced HAZ and recast layer [9]. Yet, one of the major bottlenecks of the ultrashort pulse laser system is its substantially high initial cost [10]. Further, this type of laser is relatively inefficient when used for thicker material [10].

Micro electro-discharge machining ( $\mu$ EDM), electrochemical micromachining (EMM), and micro-milling are few examples of tool-based micromachining process. Micro electro-discharge machining ( $\mu$ EDM) is a well-established technology used in the field of microfabrication because of its ability to create features in micrometers domain with high tolerance and excellent structural integrity and quality [11]. It is to note that  $\mu$ EDM is essentially an electrothermal process that utilizes repeated sparks to machine conductive materials such as metals, metallic alloys, and semiconductor with whatsoever hardness [12–14]. The  $\mu$ EDM process is free from chatter effect, mechanical stress, and vibration-related problems due to its inherent noncontact material removal mechanism [15]. Besides,  $\mu$ EDMed surface is almost free from HAZ as compared to the LBMMed ones.

Nonetheless,  $\mu$ EDM does also have various limitations. The first and foremost is its low material removal rate (MRR) [16]. Apart from low MRR, inevitable spark gap and tool wear also limit the resolution of the features fabricated by  $\mu$ EDM.

Hybrid micromachining processes have drawn particular attention by the researchers to enhance microfabrication technology as a whole [1]. The definition of hybrid machining/micromachining has differed among various researchers. According to Aspinwall et al. and Curtis et al. [17, 18], hybrid machining can be defined as the assimilation of two or more machining processes in a single machine where all the machining methods are utilized simultaneously. Menzies et al. [19] defined hybrid machining as the synergistic integration of two or more machining processes to exploit the advantages of all of them. Both EDM and laser

machining have been used in hybrid machining technology. Electrochemical discharge machining (ECDM) is one kind of hybrid machining concept where electrochemical machining and electro-discharge machining are taking place simultaneously. ECDM has the potential to be used for micromachining of nonconductive materials, unlike pure  $\mu$ EDM [20]. Electrical discharge abrasive grinding (EDAG) is another EDM-based hybrid machining that combines conventional grinding and EDM [20]. Vibration-assisted  $\mu$ EDM is another hybrid micromachining approach that has been investigated by numerous researchers [21].

Until recent years, various researchers have reported studies on laser-assisted machining processes. Singh et al. [22] proposed laser-assisted mechanical micromachining for difficult to cut materials. The laser was used to carry out the thermal softening of the hard material, while the mechanical interaction between the cutting tool and the workpiece was in progress. Sun et al. [23] proposed sequential hybrid micromachining combining LBMM and electrochemical micromachining (EMM). They [23] have successfully managed to remove the recast layer machined holes formed during the LBMM process by the subsequent EMM finishing operation. Some other reported laser-assisted machining technologies including laser-assisted turning [24], laser-assisted milling [25], and laser-assisted waterjet machining [26].

Laser- $\mu$ EDM-based sequential micromachining has also been reported by researchers [27–29]. Li et al. [27] proposed LBMM- $\mu$ EDM-based micromachining technique to produce fuel nozzle. The proposed approach helped achieve a reduction in drilling time and cost by 70% and 42%, respectively. The production capacity was also increased by 90% without compromising the hole quality than pure EDM drilling. Li et al. [27] also proposed a fixturing mechanism specific to the fuel nozzle to maintain the hole's alignment accuracy within  $\pm 20\mu$ m. Kim et al. [28] also investigated micromachining of holes and microstructures using nanosecond pulsed laser and  $\mu$ EDM. The machining time reduction was more than 50% for both micro-drilling and micro-milling operations [28]. Al-Ahmari et al. [29] investigated LBMM- $\mu$ EDM-based micro-drilling for Ni-Ti-based shape memory alloy (SMA), which helped improve the hole quality to pure LBMMed holes. A challenge for LBMM- $\mu$ EDM sequential machining is the alignment of the  $\mu$ EDM tool on the LBMMed pilot hole, which is not adequately described in the previous research [27–29]. Moreover, to the best of authors' knowledge, no study has been carried out on how the various parameters of LBMM affect the overall performance of the LBMM- $\mu$ EDM process. This work's primary motivation is to address the research gap in the field of LBMM- $\mu$ EDM-based micro-drilling, as mentioned above.

## 2 Materials and methods

This study was carried out experimentally to investigate the effect of various laser parameters on the overall performance of the LBMM- $\mu$ EDM process. Initially, sub-millimeter holes were drilled using the LBMM method with a programmed diameter of  $200\mu\text{m}$ , which was later fine finished using the  $\mu$ EDM operation. The LBMM drilling task was performed using a desktop fiber laser machine (ytterbium doped) machine (rated maximum power 20 W, actual maximum power was  $\sim 16.7$  W, measured using Gentec prento laser power meter), as shown in Fig. 1a. The laser that is used in this machine is a pulsed laser with a wavelength of 1060 nm. The focal length of this laser is 200 mm. An X/Y galvanometer scanner (maximum scan angle  $\pm 15^\circ$  and resolution  $12\ \mu\text{rad}$ ) can control the laser beam to create the various patterns on the workpiece. Figure 1b shows the scanning strategy followed during the LBMM process to make the pilot holes. The line spacing between each scan line was  $10\ \mu\text{m}$ , as indicated in Fig. 1b. The whole laser system, including the galvanometer, can be controlled using an integrated graphical user interface (GUI). Three parameters can be controlled in the LBMM system,

namely, the laser power, the pulse frequency, and the laser scanning speed, for a feature with fixed geometry. Following the LBMM drilling operation, the workpiece and the fixture were transferred to the  $\mu$ EDM machine (DT110, Fig. 1c) from Mikrottools Pte. Ltd. The  $\mu$ EDM is a CNC programmable machine that has a positional accuracy of  $\pm 1\ \mu\text{m}$  per 100 mm of travel length. The programming resolution of this machine is  $0.1\ \mu\text{m}$ . The EDM power supply of this machine is an RC pulse generator. The stray capacitance of the system was measured by monitoring the single pulse discharge energy which was found to be  $0.6\ \text{nF}$ . The material used for this study was stainless steel (SS304) with a thickness of 0.2 mm. Table 1 describes the laser and  $\mu$ EDM parameters that have been used for this research. It is to note that  $\mu$ EDM parameters were kept constant, whereas the laser parameters were varied in four stages with a full factorial experimental design.

At first, a square array of pilot holes was drilled with different laser parameters as per the experimental design. The time needed to drill each hole by the LBMM process was recorded using a stopwatch (resolution was 1/100th of a second). In the second phase, fine machining was performed on

**Fig. 1** (a) Fiber laser machining setup, (b) scanning strategy for the LBMM process, and (c)  $\mu$ EDM setup

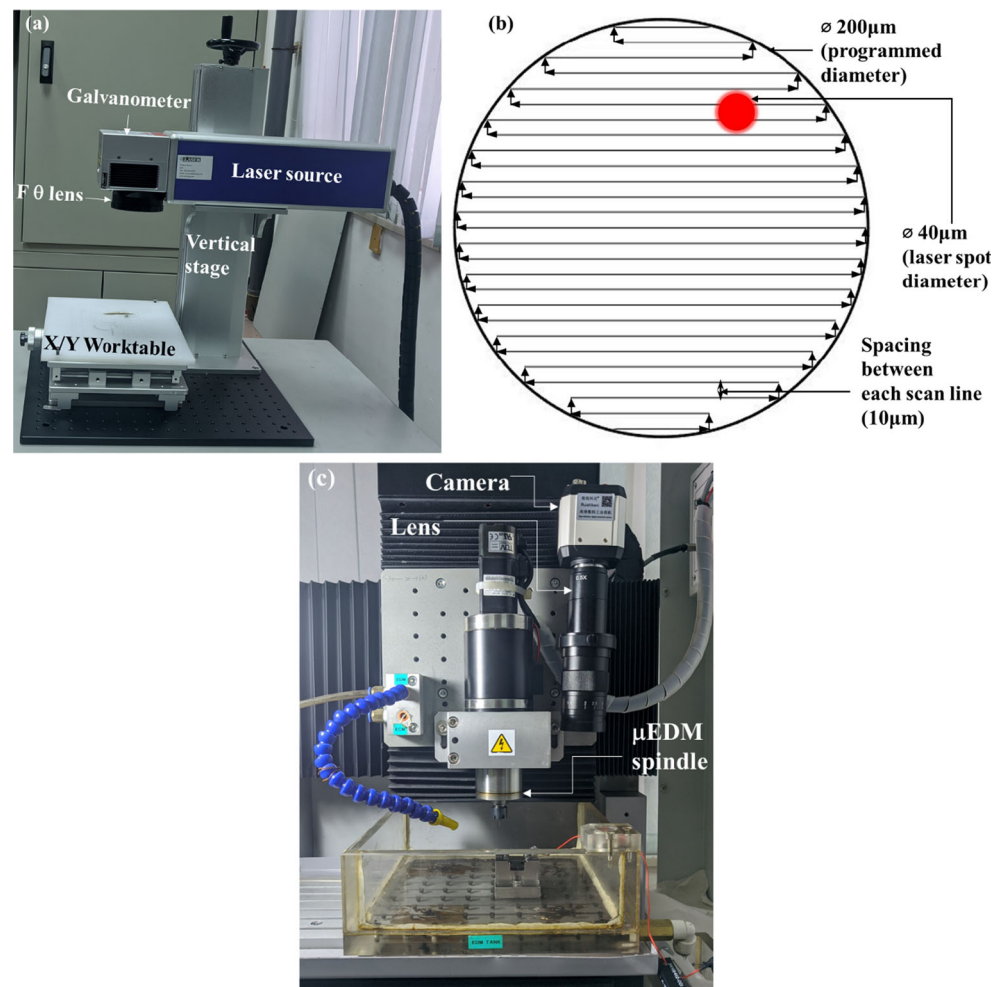


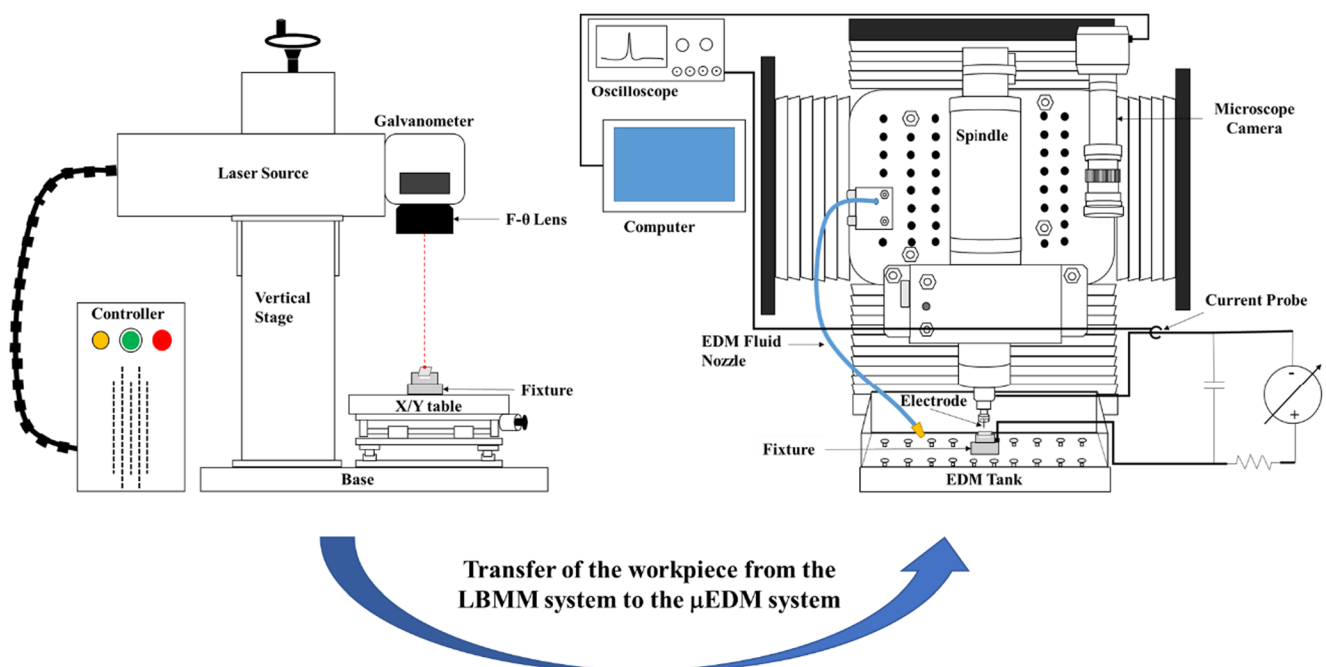
**Table 1** Various parameters for laser and  $\mu$ EDM

Parameter	Laser	$\mu$ EDM
Average power (%)	15, 40, 65, 90	-
Measured average power (W)	6.4, 9.4, 12.5, 15.5	-
Laser spot diameter ( $\mu\text{m}$ )	40	-
Laser pulse duration (ns)	100	-
Pulse frequency (kHz)	5, 10, 15, 20	-
Voltage (V)	-	80
Capacitor (nF)	-	1
Stray capacitance (nF)	-	0.6
Laser scanning speed (mm/s)/ $\mu$ EDM feed speed ( $\mu\text{m/s}$ )	50, 500, 950, 1400	5
Set diameter of the hole for laser operation ( $\mu\text{m}$ )	200	-
Electrode diameter for $\mu$ EDM ( $\mu\text{m}$ )	-	500
Loop count (Nos)	75	-
$\mu$ EDM electrode rotational speed (RPM)	-	500
$\mu$ EDM electrode material	-	Tungsten (W)

the  $\mu$ EDM (DT110) machine. Schematically the overall sequential machining process is described in Fig. 2. To carry out the fine machining by  $\mu$ EDM, a 500  $\mu\text{m}$  tungsten tool was used. To maintain the tungsten tool's positional accuracy above the laser-drilled holes, an on-machine measurement (OMM) system was developed that consists of a variable lens optical microscope equipped with a high-resolution digital camera. As described in Fig. 2, the OMM was mounted adjacent to the  $\mu$ EDM spindle.

The method that was followed to position the tungsten tool above the LBMMed holes accurately is described here. At

first, the sample workpiece was firmly attached with the fixture, and arrays of LBMMed holes were machined. Following this, the whole fixture and the workpiece were transferred to the  $\mu$ EDM (DT110) machine, and a reference hole was machined (using the  $\mu$ EDM process) near the arrays of LBMMed holes. The reference hole coordinates were made known to us from the linear scale feedback of the  $\mu$ EDM machine. Next, with the help of the camera (crosshair mark) and linear scale feedback, the deviation of X and Y coordinates for each LBMMed hole from the reference hole was measured and subsequently added to the reference hole's coordinates.

**Fig. 2** Schematic illustration of the sequential micromachining process LBMM- $\mu$ EDM



Thus, the tungsten tool was positioned right on the top of the center of the LBMMed holes for fine machining with acceptable accuracy (theoretically the accuracy is within 2  $\mu\text{m}$ ). To evaluate qualitatively the accuracy of the EDM tool's positioning method over the LBMMed holes, the  $\mu\text{EDM}$  operation was carried out on the LBMMed hole partially, and an optical image was captured (Fig. 3). It is quite clear from Fig. 3 that the  $\mu\text{EDM}$  tool could be positioned on top of the pilot holes with adequate accuracy using the developed OMM system. Next, the time needed to drill each hole (by  $\mu\text{EDM}$ ) was recorded from the machine directly without the need of a stopwatch.

The discharge current amplitude and frequency were measured using a current probe (Tektronics: Tek CT1, sensitivity 5mV/mA) as it was attached with an oscilloscope (RIGOL). During the EDM process, a short circuit may occur due to metal to metal contact, which causes no material removal [30]. When short circuit happens (which is detected by the controller of the DT110 machine by monitoring the electrical characteristics of the  $\mu\text{EDM}$  process), the machine creates a buzzer sound and causes the tool's forward motion to be reversed until an open circuit is detected again. The buzzer sound was used to count the total number of short circuits' occurrence during each  $\mu\text{EDM}$  operation. It is to note that the DT110 machine has the capability of detecting a conductive surface as soon as it touches in X, Y, or Z direction. In order to measure the vertical tool wear, the tungsten tool was moved in the negative Z direction to detect a predefined reference surface. Once the surface was detected, the Z coordinate was recorded. This operation was carried out before and after the machining of each hole. Subsequently, the difference between the two Z coordinates was calculated to find the vertical tool

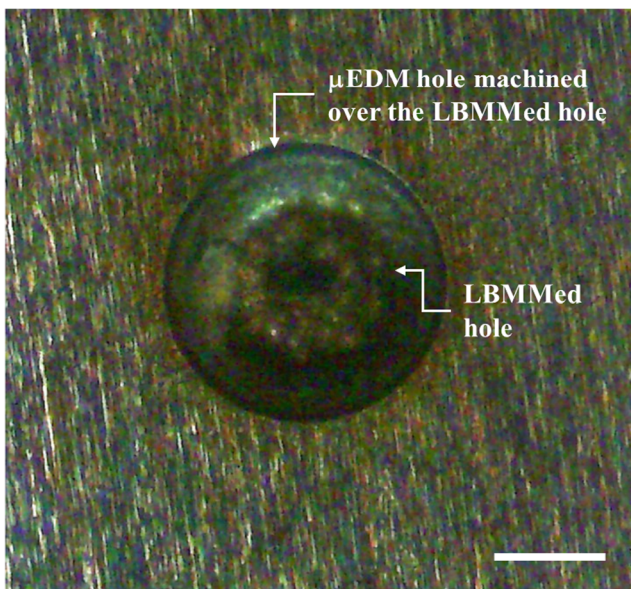


**Fig. 3** The effectiveness of the proposed centering method of the  $\mu\text{EDM}$  tool on the pre-machined LBMMed hole. Scale bar = 200 $\mu\text{m}$

wear. For,  $\mu\text{EDM}$  operation, each hole the bottom portion of the tungsten tool was flattened using a process called reverse EDM to ensure a similar tool shape for machining all the holes [31].

The characterization of the machined samples was carried out using the scanning electron microscopy (SEM: JSM-IT100 InTouch Scope<sup>TM</sup>), and the characterization was conducted two times, first after the LBMM operation and finally after the  $\mu\text{EDM}$  finishing. Once all the SEM images were captured, a third-party image analysis software (ImageJ) [32] was used to measure the holes' entry and exit areas (both for the LBMMed and the  $\mu\text{EDM}$ ed holes). The volume of material removed during the LBMM process is a crucial parameter to be measured for this study. This measurement is complicated as LBMMed holes does not have a defined circular shape, and some laser parameters used in this study was unable to penetrate a thru-hole on the workpiece. Figure 4 shows the measurement example using the image analysis software (ImageJ) [32]. Once holes' areas (entry area: Fig. 4a and c, exit/bottom area: Fig. 4b and d) and slanted height (Fig. 4e) were measured, then the removed volume by the LBMM process each hole was calculated. The hole that was formed by the LBMM process resembles the shape of a cone whose top has been sliced off. If the entry area of the hole is  $B_1$  and the exit area of the hole is  $B_2$  and the depth of the hole is  $h$ , then the formula for volume ( $V$ ) of material removed by LBMM is given by Eq. (1).

$$V = \frac{h}{3} (B_1 + \sqrt{B_1 B_2} + B_2) \quad (1)$$

It was not possible to measure the depth ( $h$ ) directly for the holes which were not fully penetrated due to the unavailability of the cross-sectional image of such holes. So, the formula for  $h$  in terms of the slanted height was derived as Eq. (2) which was used for the holes like that for Fig. 4e. However, for the case of fully penetrated holes like in Fig. 4a and b, the thickness of the workpiece was taken as  $h$ .

$$h = \sqrt{s^2 - \frac{B_1}{\pi} - \frac{B_2}{\pi} + 2 \frac{\sqrt{B_1 B_2}}{\pi}} \quad (2)$$

The abovementioned method of measuring the removed volume during the LBMM process was accurate enough to provide the average trend of material removal by the said process with the variation of laser power and scanning speed.

### 3 Results and discussions

Figure 5 provides a morphological comparison of the hole quality among the three processes used, namely, LBMM,  $\mu\text{EDM}$ , and LBMM- $\mu\text{EDM}$ . LBMM method performs the

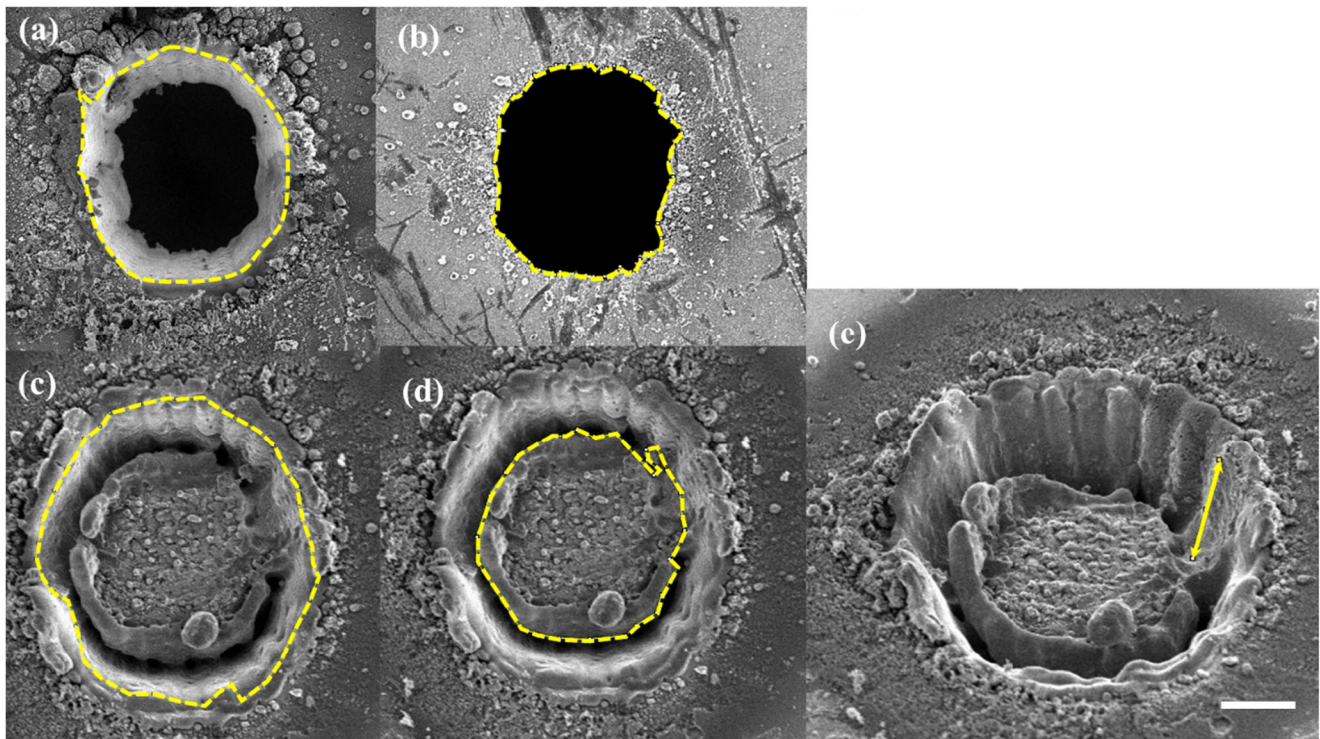


**Fig. 4** Measurement of LBMMed holes entry, exit, slanted height, and the bottom area for calculating the volume removed by the LBMM process: (a) entry area of a thru-hole, (b) exit area of a thru-hole, (c)

entry area of a blind hole, (d) bottom area of the blind hole, and (e) slanted height of the blind hole. Scale bar = 100 $\mu$ m

best in terms of machining time as it can drill the hole less than 1 min, yet, in regard to the quality of the hole, LBMM performed the worst as it resulted in a thick recast layer and low circularity. On the other hand, the quality of the holes machined by  $\mu$ EDM and LBMM- $\mu$ EDM sequential process was almost identical. However, the time taken for LBMM- $\mu$ EDM sequential process to drill the hole was virtually  $\sim 2.6$  x times lower as compared to pure  $\mu$ EDM method as shown in Fig. 6. The above findings are also in line with the

results reported by the previous researchers [29]. Figure 6 also shows that the occurrence of the short circuit during the LBMM- $\mu$ EDM process was much smaller as compared to the standard  $\mu$ EDM process ( $\sim 40$  x) which indicates that LBMM- $\mu$ EDM more stable in contrast to pure  $\mu$ EDM.

Additionally, vertical tool wear was also found to be almost  $\sim 9$  x lower for the case of the sequential micromachining. The reason for the improved machining stability and lower tool wear is because in the

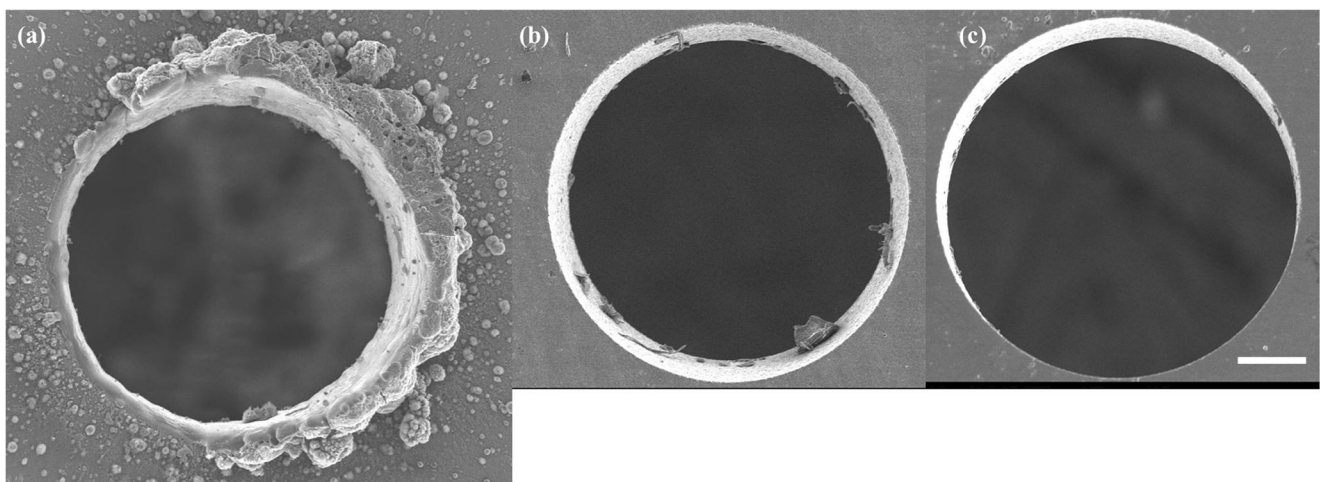
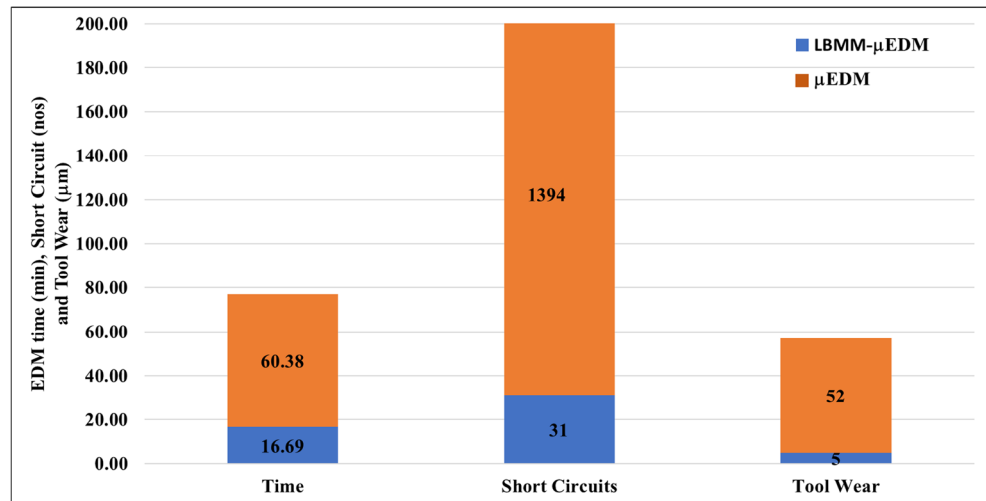


**Fig. 5** The morphological comparison of the microholes machined by (a) pure LBMM process, (b) pure  $\mu$ EDM process, and (c) LBMM- $\mu$ EDM-based sequential process. Laser processing was carried out at 15.5W laser power, 50mm/s scanning speed, and 20kHz pulse frequency. Scale bar = 100 $\mu$ m



**Fig. 6** Comparison of machining time, nos of short circuits, and tool wear between LBMM- $\mu$ EDM and pure  $\mu$ EDM

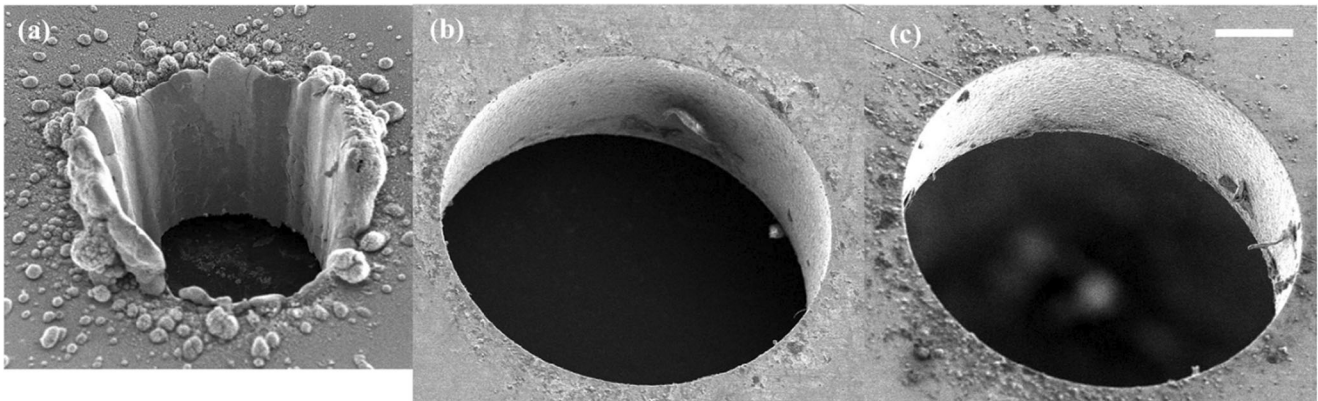


LBMM- $\mu$ EDM method, the total material to be removed from the workpiece is lesser in comparison to the pure  $\mu$ EDM. Moreover, Fig. 7 shows the tilted scanning electron microscopic views of the holes. It can be seen from Fig. 7 that pilot hole machined by the LBMM process contains significant recast layer (similar to Fig. 5) with a non-uniform inner surface (a). The recast layer can be entirely removed, and hole with a uniform inner surface can be created by the subsequent  $\mu$ EDM-based finishing operation Fig. 7b. Further to note that the quality of the LBMM- $\mu$ EDMed hole (Fig. 7b) is as good as the pure  $\mu$ EDMed hole (Fig. 7c) in terms of the inner surface uniformity and minimized recast layer. In the next sections, we will discuss how various LBMM parameters influence different performance indicators of the LBMM- $\mu$ EDM-based sequential micromachining. Among the three laser parameters that we varied in this study (pulse frequency, scanning speed, and power), pulse frequency did not show any dominant effect on the performance of the said sequential micromachining process.

### 3.1 Study of $\mu$ EDM machining time for laser- $\mu$ EDM process

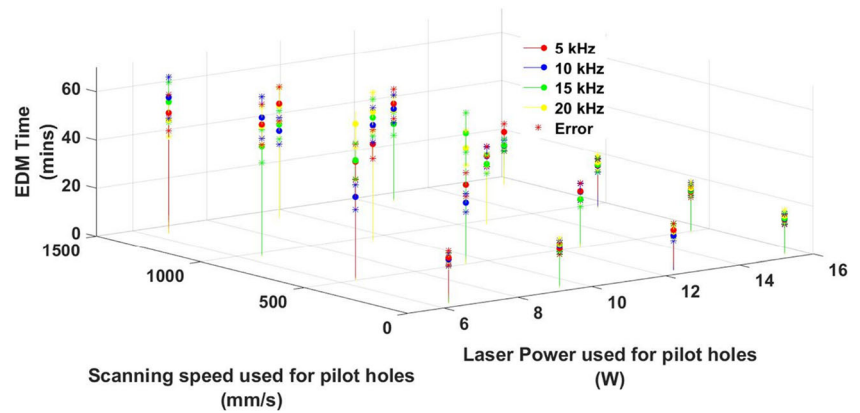
As mentioned before, this study was conducted on LBMM- $\mu$ EDM-based sequential micromachining process where the LBMM was used first followed by the  $\mu$ EDM machining to fine finish the LBMMed holes. The time for the LBMM machining was insignificant as compared to the finishing time by  $\mu$ EDM. Figure 8 demonstrates how the  $\mu$ EDM machining time is varied for the pilot holes drilled with various laser power, scanning time, and pulse frequency. Our study confirms that pulse frequency has no significant effect on the  $\mu$ EDM machining time. We observed that pilot holes machined with higher laser power and slower scanning speed require lesser time to be fine finished by  $\mu$ EDM. However, for the LBMMed holes machined with fast scanning speed, the effect is the opposite.

As the laser pulse frequency was found to have a random effect on the final machining time by  $\mu$ EDM, it was averaged up. Figure 9 shows the effect of laser power and scanning



**Fig. 7** Morphological study of the microholes (a) initially machined by the LBMM process, (b) fine finished by the  $\mu$ EDM process, and (c) fully machined by the  $\mu$ EDM process. Scale bar = 100 $\mu$ m

**Fig. 8** The effect of the incident laser power, scanning speed, and pulse frequency (used for the pilot hole machining) on the  $\mu$ EDM processing time for the final finishing of the pilot holes. The error bar represents the machining uncertainty



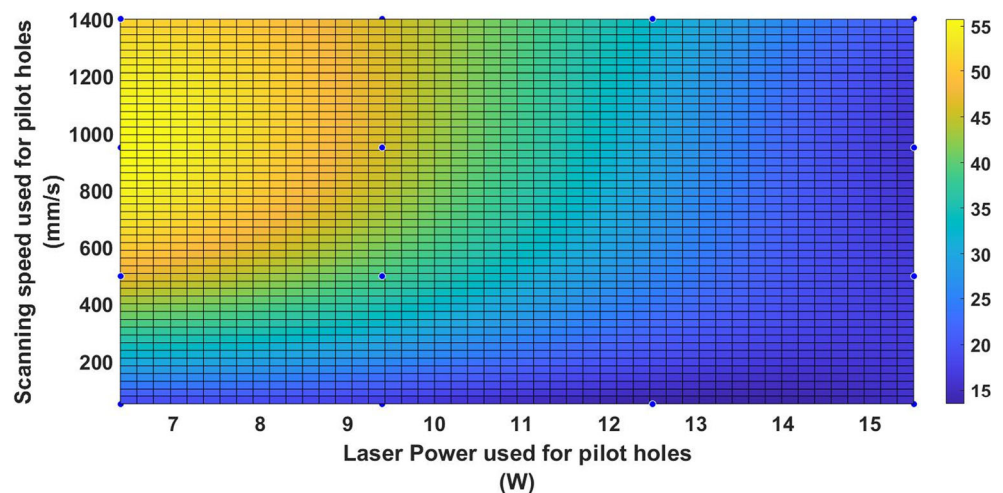
speed (with the frequency effect being averaged) on the final  $\mu$ EDM time to get more quantitative insight into the whole process. It can be inferred from Fig. 9 that if a scanning speed of less than or equal to 200 mm/s is used with any range of laser power (6.4W to 15.5W) for the LBMM operation, then final  $\mu$ EDM operation can be completed within 30 min. Further, for high laser power ( $\geq 13$  W), even the highest scanning speed can be used for the LBMM machining, yet final finishing procedure by  $\mu$ EDM can be done in less than or equal to 30 min. Figure 10 shows the average discharge frequency and discharge current measured during the  $\mu$ EDMing operation of the LBMMed holes. This figure (Fig. 10a and b) also reinforces the finding that the machinability improves for the LBMMed holes processed with higher laser power and lower scanning speed as both discharge frequency and discharge value increases due to the improvement in the ease of machining [33]. The phenomena observed in Fig. 8 and Fig. 9 can be explained from the study of the LBMMed holes entry, exit area, and removed volume during the LBMM process.

Figure 11 describes the effect of laser power and pulse frequency on the entry area of the initial holes for different laser scanning speed. It can be realized from Fig. 11a–d that

holes' entry area has an increasing trend with the laser power. However, we could not find any significant relation between the entry area and the pulse frequency of the laser. Further, Fig. 12 shows the SEM images of the holes machined at different laser power which also confirms the increasing trend in the entry area (Fig. 12a–d) with the incident laser power. On the other hand, Fig. 13 describes that higher laser scanning speed averagely causes the entry area of the LBMMed holes to be reduced. Negarestani et al. [34] stated that in the LBMM process, the incident energy density is proportional to the laser power and inversely proportional to the scanning speed. In our study, as the incident energy became higher with the increase in the laser power, the entry area of the hole was also expanded.

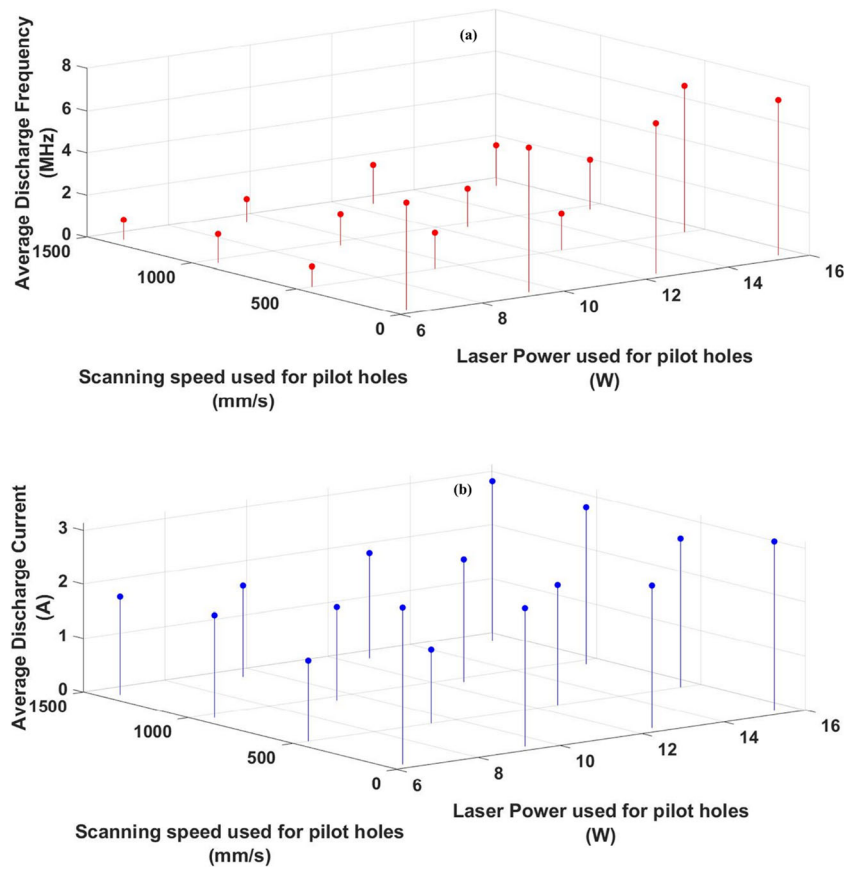
Similarly, lower energy density due to the faster scanning speed decreased the holes' entry area. Regarding the exit area of the LBMMed holes, phenomena similar to the entry area was observed, as shown in Fig. 14a–d. However, it can be said that the effect of scanning speed was found to be more dominant on the variation of the exit area as compared to the entry area, which is also visible from the SEM images, as shown in Fig. 15a–d. At a slow scanning speed like 50 mm/s, we had

**Fig. 9** The zone of faster and slower  $\mu$ EDM machining time as a function of laser incident power and laser scanning speed (used for pilot hole drilling using the LBMM process)





**Fig. 10** The average discharge current and discharge frequency variation during the  $\mu$ EDM process as a function average laser power and scanning speed used for the pilot hole machining, (a) variation of the discharge current and (b) variation of the discharge frequency



holes significantly penetrated for the whole range of power. As the scanning speed was equal or more than 500 mm/s, laser power less than or equal to 9.4W could not melt and vaporize the material enough to result in LBMMed holes with substantial exit area. Also, Fig. 16 demonstrates that the volume of

material removed during the LBMM process increases with increasing average laser power and decreases with higher scanning speed. The trend of the  $\mu$ EDM machining time observed in Fig. 8 and Fig. 9 is the effect of LBMMed holes' volume resulting from laser power and scanning speed

**Fig. 11** The effect of the incident laser power and pulse frequency on the entry area of the pilot holes machined by the LBMM process. (a) The scanning speed was at 50mm/s. (b) The scanning speed was at 500mm/s. (c) The scanning speed was at 950mm/s. (d) The scanning speed was at 1400mm/s. The loop count for all cases was 75. The error bar shows the overall uncertainty

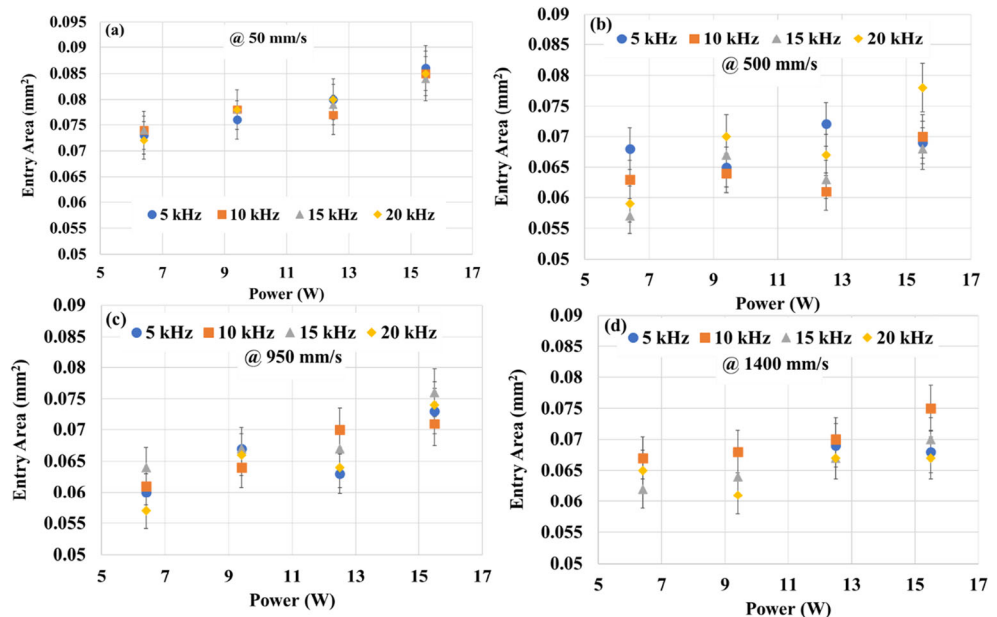
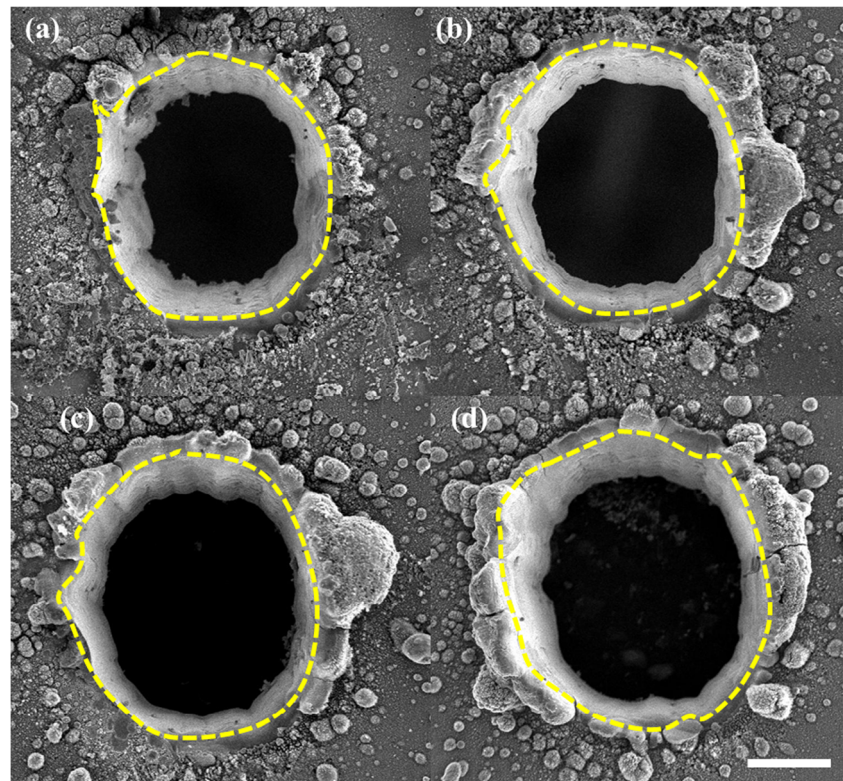


**Fig. 12** The SEM images of the entry area of the LBMMed holes machined by different incident laser power. (a) 6.4W laser power, (b) 9.4W laser power, (c) 12.5W laser power, and (d) 15.5W laser power. The loop count was 75, the scanning speed was 50mm/s, and the laser pulse frequency was 5 kHz for all the holes. Scale bar = 100 $\mu$ m. Black edge marker is used to highlight the entry area



variation. As mentioned, higher incident laser power and lower scanning speed caused significant removal of material during the pilot hole machining by the LBMM process. Therefore, during the  $\mu$ EDM operation, the machine required to remove lesser material that caused in faster processing time (Fig. 8 and Fig. 9).

### 3.2 Study of $\mu$ EDM machining stability and tool wear for laser- $\mu$ EDM process

Machining stability for the  $\mu$ EDM process (secondary operation of LBMM- $\mu$ EDM machining) is denoted by the short

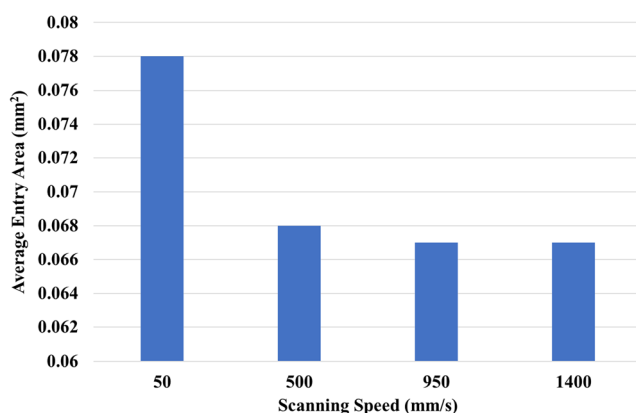
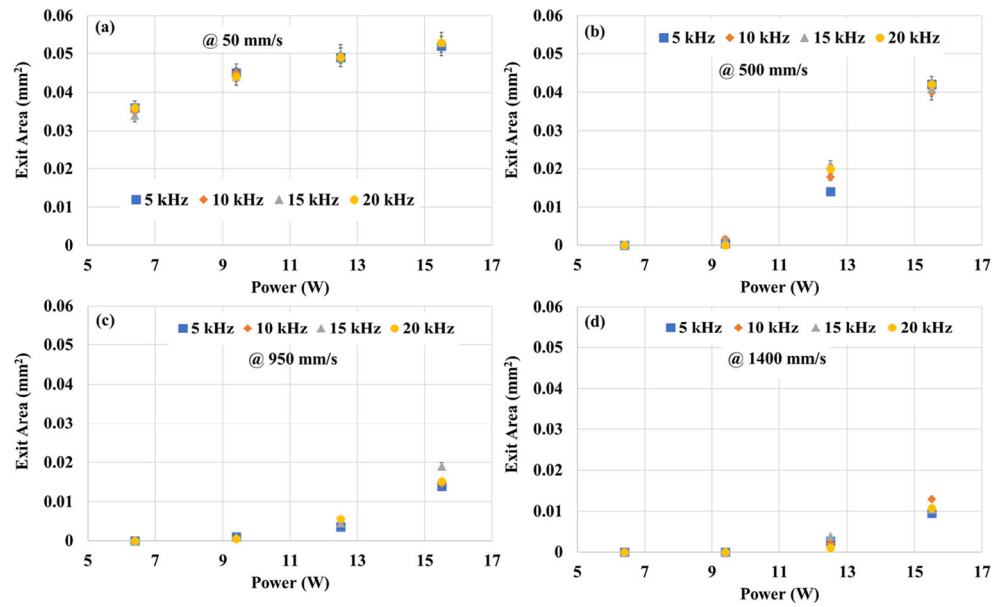


**Fig. 13** The average effect of the laser scanning speed on the entry area of the pilot holes machined by the LBMM process. All the data for each scanning speed has been averaged up to plot this graph

circuits' occurrence during the operation. The DT110  $\mu$ EDM machine is designed in such a way that if there is a detection of the short circuit during the  $\mu$ EDM process, the tool path of the electrode will be reversed to overcome the temporary short circuit condition. The  $\mu$ EDM operation is said to be unstable if too many short circuits are detected in a single machining process. As  $\mu$ EDM is an electrothermal method, it causes the electrode to be worn out also due to the repeated sparks. In this study, we have measured both the short circuit and the vertical tool wear by the method explained in section 2. As described in Fig. 17a–d, it is clear that both tool wear and short circuit during  $\mu$ EDM finishing decrease if higher laser power and slower laser scanning speed are used during the LBMM based rough drilling. This phenomenon can be explained from Fig. 18 which shows that both tool wear and number of short circuits during  $\mu$ EDM is highly correlated (positively) with the  $\mu$ EDM time with the correlation factors 0.92 (Fig. 18 a) and 0.99 (Fig. 18b), respectively. This means that higher  $\mu$ EDM time will cause more increased tool wear and short circuit occurrence due to the more extended tool and workpiece interaction. Figure 9 confirms that if higher laser power and slower scanning speed are used for LBMM drilling, then  $\mu$ EDMing time required for fine finishing of the LBMMed holes will be reduced, hence lower tool wear and short circuit occurrence during the operation. If the LBMM process uses the power of 6.4W with scanning speed as high as 1500 mm/s, then the tool wear and short circuit can go up to  $\sim$ 58  $\mu$ m and  $\sim$ 1045, respectively,

**Fig. 14** The effect of the incident laser power and pulse frequency on the exit area of the pilot holes machined by the LBMM process. (a) The scanning speed was at 50mm/s. (b) The scanning speed was at 500mm/s. (c) The scanning speed was at 950mm/s. (d) The scanning speed was at 1400mm/s. The loop count for all cases was 75. The error bar shows the overall uncertainty



which is almost similar to that of pure  $\mu$ EDM. However, if a high power of 15.5W or above is used with any range of scanning speed, then the tool wear and the number of the short circuit will be around  $\sim 10 \mu\text{m}$  and  $\sim 100$ , respectively, which is substantially reduced than the pure  $\mu$ EDM (Fig. 6). Figure 19 a–b further confirm that not only the total tool wear and total short circuits but also the average rate of tool wear and the average rate of the short circuit also significantly influenced by the laser input parameters that are used for the pilot hole machining. The rate of tool wear and short circuit during the  $\mu$ EDM process can go up to as high as  $1 \mu\text{m}/\text{min}$

and 20nos/min if high laser scanning speed is used at a low laser incident power during the LBMM process. When low laser power and high scanning speed are used during the LBMM method, then the volumetric size of the LBMMed pilot holes become smaller (Fig. 16). Hence, at the time of  $\mu$ EDM, the tool needs to remove more material from the workpiece, which resulted in more debris formation. As a result, the rate of short circuit and tool wear also increases, whereas for the case of LBMMed holes with more volume of material removed requiring less material to be removed by the  $\mu$ EDM operation, hence we observed more frequent sparking

**Fig. 15** The effect of the incident laser scanning speed on the exit area of the pilot holes machined by the LBMM process. (a) 50 mm/s laser scanning speed, (b) 500 mm/s laser scanning speed, (c) 950 mm/s laser scanning speed, and (d) 1400 mm/s laser scanning speed. The loop count was 75, the incident laser power was 6.4W, and the laser pulse frequency was 15 kHz for all the holes. Scale bar =  $100 \mu\text{m}$

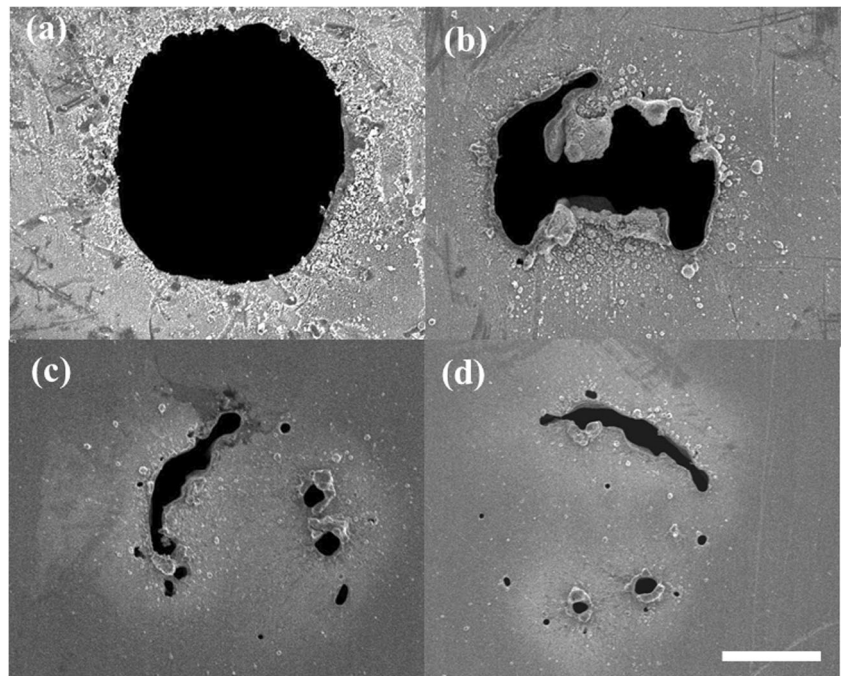
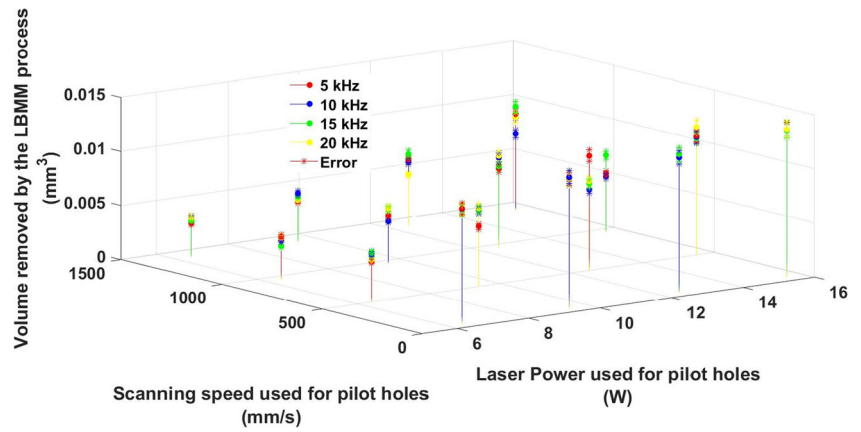




**Fig. 16** The volume of material removed by the LBMM process as a function of average laser power and scanning speed



and high discharge current (by monitoring the discharge current) during the process. Therefore, the rate of short circuits occurrence and tool wear decreased.

### 3.3 Study of residual spatter zone for laser-μEDM process

It is expected that during the sequential LBMM-μEDM micromachining, the zone with residual spatter resulted from the LBMM process [35] should be removed entirely. However, we have seen from our study that if high laser power (15.5W) with low scanning speed is used for the pilot hole drilling (using LBMM) with the currently programmed diameter of 200 μm, then μEDM process may not be able to remove the zone with spatter completely. This problem can be solved in two ways: in the first method, the sample plate can

be cleaned with isopropyl alcohol (IPA) wipe followed by cleaning in an ultrasonic bath as suggested by Schaeffer et al. [36]. In the second method, the programmed diameter of the LBMM process could be optimized in such a way that finishing operation by μEDM could altogether remove the residual spatter zone from the surface as generated by the LBMM. We experimentally tried several diameters and found out that if 100 μm is used for the LBMM (laser power 6.4W, scanning speed 200 mm/s, pulse frequency 20 kHz), then μEDM could completely remove the residual spatter zone. Figure 20 shows the comparison between the two holes machined with μEDM and LBMM-μEDM process. It is quite clear from the two pictures (Fig. 20) that both the holes are completely clean from any spatter at the surroundings of the holes. It is obvious that by reducing the LBMMed diameter to a half, the performance parameter of the μEDM process is

**Fig. 17** The variation of average tool wear and number of the short circuit during the μEDM process as a function the incident laser power used for the pilot holes drilling. (a) The scanning speed was at 50mm/s. (b) The scanning speed was at 500mm/s. (c) The scanning speed was at 950mm/s. (d) The scanning speed was at 1400mm/s. The loop count was 75 for all the cases

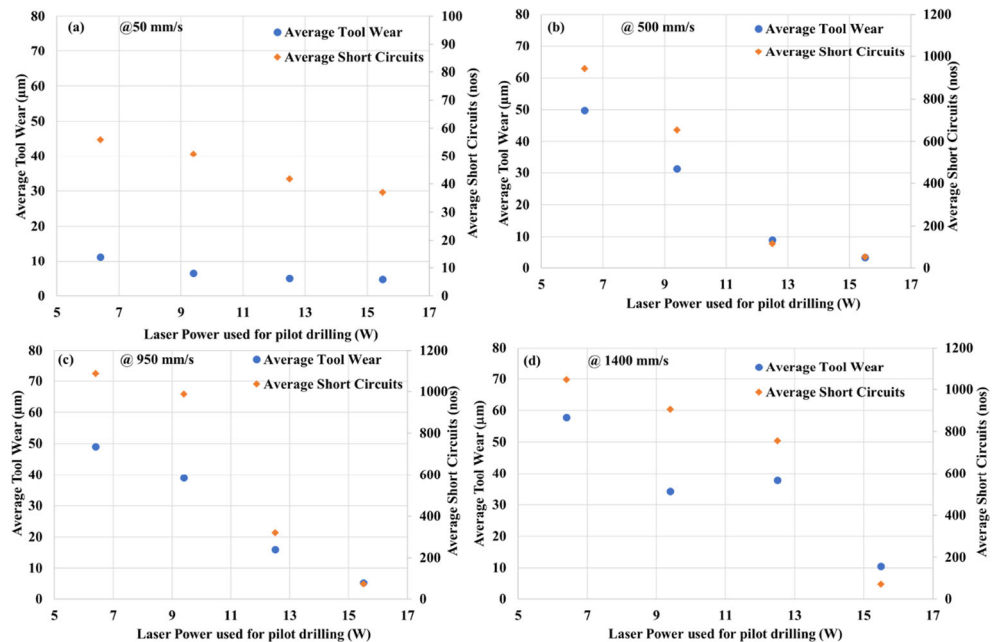
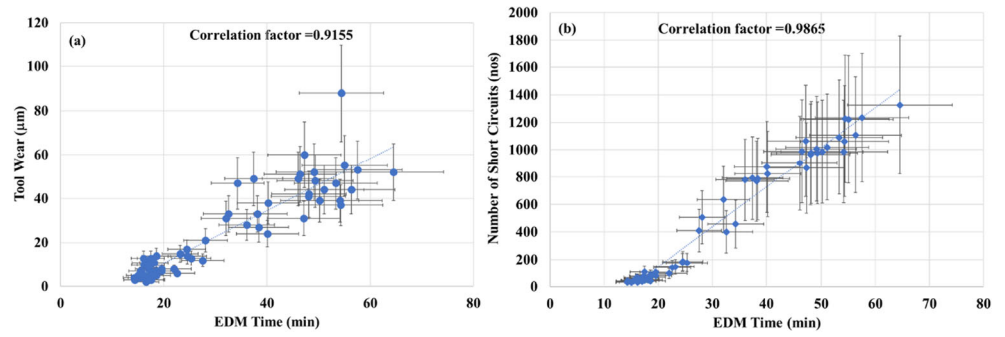


**Fig. 18** The correlation between tool wear and short circuits vs  $\mu$ EDM time. **(a)** Tool wear vs  $\mu$ EDM time. **(b)** Short circuits vs  $\mu$ EDM time. Error bar shows the experimental variation



compromised. However, it is still significantly better than the pure  $\mu$ EDM as described in Fig. 20 which shows that machining time, tool wear, and short circuit occurrence were improved by 95%, 4 x, and 2.5 x, respectively.

The choice between the two processes (IPA wipe and ultrasonic bath or reducing the LBMMed hole size) for complete removal of the residual spatter depends on the user’s preference. If the users go for IPA wipe and ultrasonic bath-based cleaning technique, then they can go for aggressive parameters during the LBMM process, i.e., higher programmed diameter and high laser power. However, if the users do not have the facilities mentioned above, then they need to choose a lower diameter for the LBMM process with lower power and elevated scanning speed.

### 4 Conclusion

In this study, we have investigated how different laser parameters affect the various performance indicators of the LBMM- $\mu$ EDM-based sequential micromachining process. We observed that LBMM- $\mu$ EDM process could help to lower the production time of the microhole fabrication by a margin of  $\sim 2.65$  x as compared to pure  $\mu$ EDM, yet maintaining the same quality of the machined hole in terms of free of recast layer, circularity, etc. Concerning the machining time, we found that high laser power and slow scanning speed to produce the pilot holes (as compared to low laser power and fast scanning speed) help to lower the machining time by the  $\mu$ EDM process, up to 250%. We also observed that the tool

**Fig. 19** The average tool wear rate and the short circuit occurrence rate as a function of laser incident power and laser scanning speed (used for pilot hole drilling using the LBMM process). **(a)** Rate of tool wear and **(b)** rate of short circuit occurrence

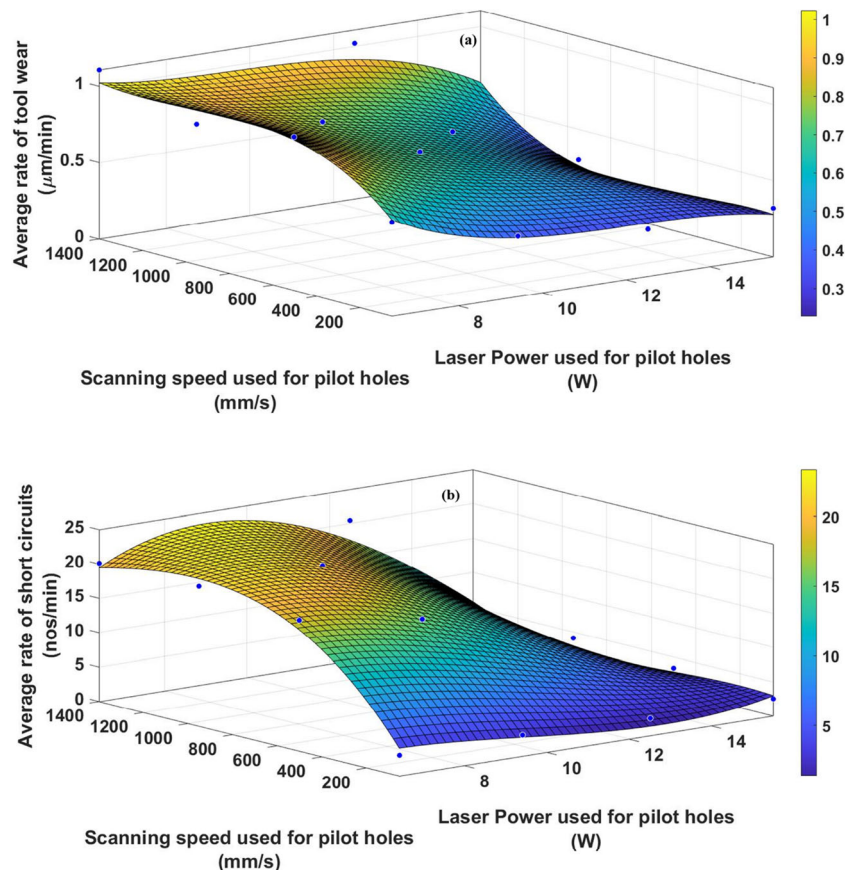
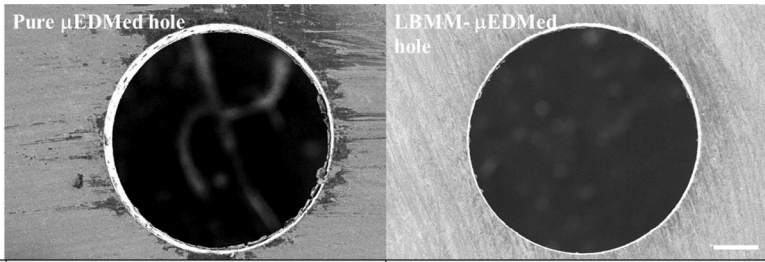


**Fig. 20** Comparison between pure  $\mu$ EDMed hole and LBMM- $\mu$ EDMed holes. Both holes confirm that there is no residual spatter zone present on the surrounding of the hole. Scale bar = 100 $\mu$ m



$\mu$ EDM time	61.26	31.35 (improved by more than 95%)
Tool wear ( $\mu$ m)	73	14 (improved by more than 400%)
Short Circuits Count (nos)	1327	367 (improved by more than 250%)

wear and short circuit occurrence during the  $\mu$ EDM process were significantly affected by the size of the LBMMed holes machined by various LBMM parameters. High tool wear rate and short circuit rate were observed ( $\sim 1\mu\text{m}/\text{min}$  and  $\sim 20\text{nos}/\text{min}$ , respectively) during the  $\mu$ EDM operation if low laser power and high scanning speed were used for the LBMMed holes. Finally, we observed that the residual spatter zone resulted from the LBMM process could be entirely removed by the  $\mu$ EDM process if the programmed diameter for the LBMM process was halved. As a result, the LBMM- $\mu$ EDM performance was compromised in terms of machining time, tool wear, and short circuit occurrence; however, they were yet considerably better than pure  $\mu$ EDM process.

**Acknowledgement** First of all, we thank Allah (SWT) for providing us with the ability to conduct this research. The authors also acknowledge the research support provided by the International Islamic University Malaysia. We also thank the Ministry of Higher Education Malaysia and the Asian Office of Aerospace Research and Development for their generous funding to carry out this research.

**Author contribution** Mir Akmam Noor Rashid and Wazed Ibne Noor are the graduate students involved in this project who actively carried out the experiments, characterizations, compilation, and analysis of the data. Mir Akmam Noor Rashid mostly contributed to drafting the article. Tanveer Saleh is the principal investigator of the projects who conceptualized the whole research problems. He is the main supervisor of the above students and guided them during experimentation and data analysis. Mohamed Sultan Mohamed Ali is one of the research collaborators who provided crucial technical input on the manuscript.

**Funding** This project was funded by research grants provided by the Ministry of Higher Education Malaysia (MOHE Grant No: FRGS/1/2018/TK03/UIAM/02/2) and Asian Office of Aerospace Research and Development (AOARD Grant No: BAA-AFRL-AFOSR-2016-0007). In particular, Mir Akmam Noor Rashid was paid as a graduate research assistant (GRA) from the MOHE grant, and Wazed Ibne Noor was paid as a graduate research assistant from the AOARD grant.

**Availability of data and materials** Not applicable

## Declarations

**Ethics approval** This paper does not require any ethical approval as the study does not involve human participants or animals.

**Consent to participate** Not applicable as this work does not involve human subjects.

**Consent to publish** Not applicable as this work does not involve human subjects.

**Competing interests** The authors declare no competing interests.

## References

- Chavoshi SZ, Luo X (2015) Hybrid micro-machining processes: a review. *Precis Eng* 41:1–23. <https://doi.org/10.1016/j.precisioneng.2015.03.001>
- Rahman M, Asad ABMA, Masaki T, Saleh T, Wong YS, Kumar AS (2010) A multiprocess machine tool for compound micromachining. *Int J Mach Tools Manuf* 50:344–356
- Liu Y, Zhu D, Zeng Y, Yu H (2011) Development of microelectrodes for electrochemical micromachining. *Int J Adv Manuf Technol* 55:195–203. <https://doi.org/10.1007/s00170-010-3035-2>
- Mishra S, Yadava V (2015) Laser beam micromachining (LBMM) - A review. *Opt Lasers Eng* 73:89–122. <https://doi.org/10.1016/j.optlaseng.2015.03.017>
- Ghosal A, Manna A, Lall AK (2014) Modelling of ytterbium fiber laser parameters during micro machining of Al-15 wt%Al<sub>2</sub>O<sub>3</sub>-MMC. *Procedia Eng* 90:704–709. <https://doi.org/10.1016/j.proeng.2014.11.799>
- Ancona A, Döring S, Jauregui C, Röser F, Limpert J, Nolte S, Tünnermann A (2009) Femtosecond and picosecond laser drilling of metals at high repetition rates and average powers. *Opt Lett* 34:3304–3306. <https://doi.org/10.1364/ol.34.003304>
- Gruner A, Schille J, Loeschner U (2016) Experimental study on micro hole drilling using ultrashort pulse laser radiation. *Phys Procedia* 83:157–166. <https://doi.org/10.1016/j.phpro.2016.08.030>
- Barthels T, Reininghaus M, Westergeling H (2019) High-precision ultrashort pulsed laser drilling of micro and nano holes using multibeam processing. In: Dudley A, Laskin A V. (eds) *Laser Beam Shaping XIX*. SPIE, p 19
- Casalino G, Losacco AM, Arnesano A, Facchini F, Pierangeli M, Bonserio C (2017) Statistical analysis and modelling of an Yb: KGW femtosecond laser micro-drilling process. *Procedia CIRP* 62:275–280. <https://doi.org/10.1016/j.procir.2016.06.111>
- Ultrafast lasers offer great promise as a unique manufacturing tool | Industrial Laser Solutions. <https://www.industrial-lasers.com/home/article/16490420/ultrafast-lasers-offer-great-promise-as-a-unique-manufacturing-tool>. Accessed 19 Jan 2021
- Rajurkar KP, Sundaram MM, Malshe AP (2013) Review of electrochemical and electrodischarge machining. *Procedia CIRP* 6:13–26. <https://doi.org/10.1016/j.procir.2013.03.002>



12. Abu Qudeiri JE, Saleh A, Ziout A, Mourad AHI, Abidi MH, Elkaseer A (2019) Advanced electric discharge machining of stainless steels: assessment of the state of the art, gaps and future prospect. *Materials* (Basel) 16. <https://doi.org/10.3390/ma12060907>
13. Abidi MH, Al-Ahmari AM, Siddiquee AN, Mian SH, Khan MM, Rasheed MS (2017) An investigation of the micro-electrical discharge machining of nickel-titanium shape memory alloy using grey relations coupled with principal component analysis. *Metals* (Basel) 7:1–15. <https://doi.org/10.3390/met7110486>
14. Jahan MP, Lieh TW, Wong YS, Rahman M (2011) An experimental investigation into the micro-electrodischarge machining behavior of p-type silicon. *Int J Adv Manuf Technol* 57:617–637. <https://doi.org/10.1007/s00170-011-3302-x>
15. Jahan MP, Rahman M, Wong YS (2011) A review on the conventional and micro-electrodischarge machining of tungsten carbide. *Int J Mach Tools Manuf* 51:837–858. <https://doi.org/10.1016/j.ijmactools.2011.08.016>
16. Dilip DG, Panda S, Mathew J (2020) Characterization and parametric optimization of micro-hole surfaces in micro-EDM drilling on Inconel 718 superalloy using genetic algorithm. *Arab J Sci Eng* 45: 5057–5074. <https://doi.org/10.1007/s13369-019-04325-4>
17. Aspinwall DK, Dewes RC, Burrows JM, Paul MA (2001) Hybrid high speed machining (HSM): system design and experimental results for grinding / HSM and EDM / HSM. *CIRP Ann - Manuf Technol* 50:145–148. [https://doi.org/10.1016/S0007-8506\(07\)62091-5](https://doi.org/10.1016/S0007-8506(07)62091-5)
18. Curtis DT, Soo SL, Aspinwall DK, Sage C (2009) Electrochemical superabrasive machining of a nickel-based aeroengine alloy using mounted grinding points. *CIRP Ann - Manuf Technol* 58:173–176. <https://doi.org/10.1016/j.cirp.2009.03.074>
19. Menzies I, Koshy P (2008) Assessment of abrasion-assisted material removal in wire EDM. *CIRP Ann - Manuf Technol* 57:195–198. <https://doi.org/10.1016/j.cirp.2008.03.135>
20. Shrivastava PK, Dubey AK (2014) Electrical discharge machining-based hybrid machining processes: a review. *Proc Inst Mech Eng Part B J Eng Manuf* 228:799–825. <https://doi.org/10.1177/0954405413508939>
21. Maity KP, Choubey M (2019) A review on vibration-assisted EDM, micro-EDM and WEDM. *Surf. Rev. Lett.* 26:1830008
22. Singh R, Melkote SN (2007) Characterization of a hybrid laser-assisted mechanical micromachining (LAMM) process for a difficult-to-machine material. *Int J Mach Tools Manuf* 47:1139–1150. <https://doi.org/10.1016/j.ijmactools.2006.09.004>
23. Sun A, Chang Y, Liu H (2018) Metal micro-hole formation without recast layer by laser machining and electrochemical machining. *Optik* (Stuttg) 171:694–705. <https://doi.org/10.1016/j.ijleo.2018.06.099>
24. Arrizubieta JI, Klocke F, Gräfe S, Arntz K, Lamikiz A (2015) Thermal simulation of laser-assisted turning. *Procedia Eng* 132: 639–646. <https://doi.org/10.1016/j.proeng.2015.12.542>
25. Ding H, Shen N, Shin YC (2012) Thermal and mechanical modeling analysis of laser-assisted micro-milling of difficult-to-machine alloys. *J Mater Process Technol* 212:601–613. <https://doi.org/10.1016/j.jmatprotec.2011.07.016>
26. Feng S, Huang C, Wang J, Jia Z (2019) Materials science in semiconductor processing surface quality evaluation of single crystal 4H-SiC wafer machined by hybrid laser-waterjet : Comparing with laser machining. 93:238–251
27. Li L, Diver C, Atkinson J, Giedl-Wagner R, Helml HJ (2006) Sequential laser and EDM micro-drilling for next generation fuel injection nozzle manufacture. *CIRP Ann - Manuf Technol* 55:179–182. [https://doi.org/10.1016/S0007-8506\(07\)60393-X](https://doi.org/10.1016/S0007-8506(07)60393-X)
28. Kim S, Kim BH, Chung DK, Shin HS, Chu CN (2010) Hybrid micromachining using a nanosecond pulsed laser and micro EDM. *J Micromech Microeng* 20:20. <https://doi.org/10.1088/0960-1317/20/1/015037>
29. Al-Ahmari AMA, Rasheed MS, Mohammed MK, Saleh T (2015) A hybrid machining process combining micro-EDM and laser beam machining of nickel–titanium-based shape memory alloy. *Mater Manuf Process* 31:447–455. <https://doi.org/10.1080/10426914.2015.1019102>
30. Yeo SH, Aligiri E, Tan PC, Zarepour H (2009) A new pulse discriminating system for Micro-EDM. *Mater Manuf Process* 24: 1297–1305. <https://doi.org/10.1080/10426910903130164>
31. Singh AK, Patowari PK, Deshpande NV (2017) Effect of tool wear on microrods fabrication using reverse  $\mu$ EDM. *Mater Manuf Process* 32:286–293. <https://doi.org/10.1080/10426914.2016.1198015>
32. ImageJ. <https://imagej.nih.gov/ij/index.html>. Accessed 10 Sep 2019
33. Mahardika M, Tsujimoto T, Mitsui K (2008) A new approach on the determination of ease of machining by EDM processes. *Int J Mach Tools Manuf* 48:746–760. <https://doi.org/10.1016/j.ijmactools.2007.12.012>
34. Negarestani R, Li L (2012) Laser machining of fibre-reinforced polymeric composite materials. *Machining Technology for Composite Materials*. Elsevier, In, pp 288–308
35. Demir AG, Previtali B, Bestetti M (2010) Removal of spatter by chemical etching after microdrilling with high productivity fiber laser. *Phys Procedia* 5:317–326. <https://doi.org/10.1016/j.phpro.2010.08.152>
36. Schaeffer RD, Kardos G (2008) Post-laser processing cleaning techniques | industrial laser solutions. <https://www.industrial-lasers.com/drilling/article/16485770/postlaser-processing-cleaning-techniques>. Accessed 11 Oct 2020

**Publisher's note** Springer Nature remains neutral with regard to jurisdictional claims in published maps and institutional affiliations.